

## RESSALVA

Atendendo a solicitação do autor, Bruno Cavenaghi Campos, o texto completo deste documento será disponibilizado somente a partir de 28/02/2027.



UNIVERSIDADE ESTADUAL PAULISTA  
"JÚLIO DE MESQUITA FILHO"  
Campus de Bauru

Bruno Cavenaghi Campos

INVESTIGATION OF GROUND VIBRATION MEASUREMENTS FOR LEAK  
DETECTION IN BURIED WATER PIPES BY USING CAMERAS

Bauru

2025

Bruno Cavenaghi Campos

**Investigation of ground vibration measurements for  
leak detection in buried water pipes using cameras**

Dissertação apresentada à  
Faculdade de Engenharia de  
Bauru, Programa de Pós-  
Graduação em Engenharia  
Mecânica na Área de Projetos  
Mecânicos, como parte dos  
requisitos necessários à obtenção  
de Título de Mestre em Engenharia  
Mecânica.

Orientador: Prof. Dr. Fabricio Cesar Lobato de Almeida

Financiadora: FAPESP – Proc. 2022/07586-0

Bauru  
2025

C198i

Campos, Bruno Cavenaghi

INVESTIGATION OF GROUND VIBRATION  
MEASUREMENTS FOR LEAK DETECTION IN BURIED WATER  
PIPES BY USING CAMERAS / Bruno Cavenaghi Campos. -- , 2025  
82 p. : il., tabs., fotos

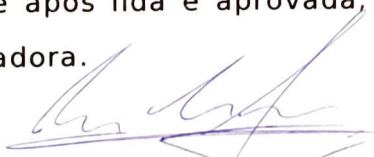
Dissertação (mestrado) - Universidade Estadual Paulista (UNESP),  
Faculdade de Engenharia, Bauru,

Orientador: Fabricio Cesar Lobato de Almeida

1. Leak Localization. 2. Computer Vision. 3. Vibration analysis. I.  
Título.

**ATA DA DEFESA PÚBLICA DA DISSERTAÇÃO DE MESTRADO DE BRUNO CAVENAGHI CAMPOS, DISCENTE DO PROGRAMA DE PÓS-GRADUAÇÃO EM ENGENHARIA MECÂNICA, DA FACULDADE DE ENGENHARIA - CÂMPUS DE BAURU.**

Aos 27 dias do mês de fevereiro do ano de 2025, às 14h, por meio de Videoconferência, realizou-se a defesa de DISSERTAÇÃO DE MESTRADO de BRUNO CAVENAGHI CAMPOS, intitulada **INVESTIGATION OF GROUND VIBRATION MEASUREMENTS FOR LEAK DETECTION IN BURIED WATER PIPES BY USING CAMERAS**. A Comissão Examinadora foi constituída pelos seguintes membros: Prof. Dr. FABRICIO CESAR LOBATO DE ALMEIDA (Orientador(a) - Participação Presencial) do(a) Departamento de Engenharia Mecânica / Universidade Estadual Paulista Unesp Faculdade de Engenharia Câmpus Bauru, Prof. Dr. FABIO MAZZARIOL SANTICIOLLI (Participação Presencial) do(a) Departamento de Engenharia Mecânica / Universidade Estadual Paulista, Prof. Dr. MARCELO AMORIM SAVI (Participação Virtual) do(a) COPPE - Engenharia Mecânica / Universidade Federal do Rio de Janeiro - UFRJ. Após a exposição pelo mestrando e arguição pelos membros da Comissão Examinadora que participaram do ato, de forma presencial e/ou virtual, o discente recebeu o conceito final: APROVADO. Nada mais havendo, foi lavrada a presente ata, que após lida e aprovada, foi assinada pelo(a) Presidente(a) da Comissão Examinadora.



Prof. Dr. FABRICIO CESAR LOBATO DE ALMEIDA

## **ACKNOWLEDGEMENTS**

I thank God for the strength and wisdom to complete this stage, my family and friends who have always encouraged me, and my fellow professors and researchers from various institutions for their support during this period.

I would like to thank my advisor Professor Dr. Fabricio Cesar Lobato de Almeida for his incentive, dedication, and knowledge in developing this work.

To UNESP, for its support and infrastructure, to the graduate program, and to everyone who helped in any way with this work.

I would like to thank FAPESP for awarding me a research grant under process no. 2022/07586-0 and 2023/03035-1.

## ABSTRACT

Leaking pipes pose a significant threat to sustainable practices in the modern world, as substantial volumes of water are lost between treatment facilities and end-users. This not only wastes valuable water resources but also results in considerable energy losses associated with pumping and treatment processes. To address this issue, water companies deploy various devices to detect leaks within their distribution networks. Among these devices are tools that leverage the vibro-acoustic characteristics of leak noise to detect and pinpoint leak locations. Examples include listening sticks/rods, geophones, and leak noise correlators, being the latter a widely used tool for precise leak localization, requiring complex signal processing. Leak noise correlators rely on at least two sensors placed onto the vibrating pipe system to estimate the time delay between signals and determine the leak position, provided the leak noise velocity is known beforehand. However, these devices are based on contact measurements, which can be challenging in scenarios where access to buried pipes is limited or when hydrometers and hydrants are inaccessible, as is often the case in Brazil. To overcome these challenges, this work investigates the use of cameras as non-contact sensors by employing computer vision techniques. A key advantage of this approach is that any pixel in the camera's field of view can serve as a measurement point (sensor). This method is particularly relevant for scenarios where achieving a low Signal-to-Noise Ratio (SNR) is crucial, as leak vibration amplitudes are typically small and can be masked by instrument and background noise. Therefore, this study outlines a systematic procedure to achieve a sufficiently low SNR using standard cameras, enabling single-point (amplitude-only) or multi-point (amplitude and phase) measurements via Optical Flow techniques for displacement tracking. The developed procedure was evaluated on a bespoke test bench designed to simulate controlled leak conditions. Results demonstrated the feasibility of using the proposed technique to track leak noise at low frequencies, constrained by the camera's frame rate. Additionally, ground vibration measurements were conducted to localize actual leak noise sources. The results are promising, indicating that phase measurements obtained through this technique can be effectively used to estimate leak locations.

**Keywords:** Leak Localization, Computer Vision, Vibration analysis.

## RESUMO

Vazamentos de água representam uma ameaça à sustentabilidade no mundo moderno, já que um volume substancial de água é perdido entre as instalações de tratamento e os usuários finais, resultando em um grande desperdício de energia para bombeamento e procedimentos de tratamento. Para enfrentar esse desafio, as empresas de água utilizam diversos dispositivos para detectar vazamentos em suas redes. Entre esses dispositivos estão aqueles que utilizam as características vibro-acústicas do ruído do vazamento para localizar sua posição. Os dispositivos mais comuns são a haste de escuta, geofone, e correlacionador de ruído de vazamento, sendo este último uma ferramenta amplamente utilizada para determinar a posição do vazamento, mas que apresenta um complexo de processamento de sinal. Além disso, os correlacionadores de ruído utilizam pelo menos dois sensores ao longo da tubulação, de modo que o atraso temporal entre os sensores possa ser estimado e a posição do vazamento seja determinada, quando a velocidade do ruído de vazamento é conhecida/estimada a priori. Medidas de contato são utilizadas para qualquer um desses dispositivos, o que pode ser difícil quando o acesso à tubulação enterrada é limitado ou quando hidrômetros/hidrantes estão fora de alcance, o que é comum no Brasil. Portanto, este trabalho tem como objetivo investigar o uso de câmeras como alternativa para medidas não contato utilizando técnicas de visão computacional. Além do mais, cada pixel pode ser tratado como uma posição de medição (sensor), o que pode ser vantajoso para detecção de vazamentos. Essa técnica é viável quando se alcança uma baixa relação sinal-ruído (SNR), já que a amplitude da vibração do vazamento é muito pequena e pode ser corrompida pelo ruído de instrumentação ou ruído de fundo. Portanto, um procedimento sistemático para obter um SNR suficientemente baixo para câmeras comuns é descrito neste trabalho, de modo que a medição de ponto único (amplitude) ou de múltiplos pontos (amplitude e fase) possa ser realizada utilizando métodos de rastreamento de deslocamento. O procedimento desenvolvido é então utilizado para mostrar a viabilidade de detectar vazamentos usando uma banca de testes, onde condições específicas podem ser simuladas. Foi demonstrado que a técnica desenvolvida pode rastrear o ruído do vazamento em baixas frequências. Além disso, medidas reais da fonte de ruído do vazamento usando vibrações de superfície foram feitas para mostrar a viabilidade da técnica. Os resultados são promissores, de modo que a fase medida pode ser usada para estimar a localização do vazamento.

**Palavras-chave:** Localização de Vazamentos, Rastreamento com câmera, Análise de Vibração

## LIST OF ILLUSTRATIONS

Figure 1: Illustration of the constant intensity assumption for Optical Flow calculation. .....	25
Figure 2: Optical Flow indication (green arrows) of some points over a surface for different frames of a video.....	26
Figure 3: Edge representation, the graph of the intensity change in the x direction, and the derivative (gradient) of the pixel intensity variation. ....	26
Figure 4: (a) Original video frame, (b) Result of the Sobel operator in the y direction, (c) Result of the Sobel operator in the x direction, (d) Result of the Sobel operator in the x and y direction simultaneously.....	27
Figure 5: Convolution process of one pixel of the image. ....	28
Figure 6: (a) Artificial video with one corner being tracked, (b) Artificial video with all corners being tracked.....	29
Figure 7: (a) Real and Tracked displacement from one corner of the white square, (b) Variation on the tracked position between frames with an average of 0.018 pixels, (c) Real and Tracked displacement from all corners of the white square, (d) Variation on the tracked position between frames with an average of 0.009 pixels.....	30
Figure 8: Examples of different color contrasts. Color distances: (a) 1, (b) 0.7, (c) 0.3, and (d) 0.05. ....	34
Figure 9: Maximum coherence value between displacement signals extracted from the artificial video for each normalized color distance value.....	35
Figure 10: (a) Photo of the experiment setup. (b) Sketch of the experiment showing the angle being changed .....	35
Figure 11: (a) PSDs of the extracted shaker signals from the camera at 0° (red), 30°(green), 60°(blue) and 90°(yellow), and accelerometer (black), (b) Coherence and (c) Unwrapped phase plots between two regions of the shaker surface for each angle.....	37
Figure 12: Videos Frames from the (a) ISO 200 and (b) ISO 12800 videos. ....	38
Figure 13: (a) Time domain signals filtered between 20Hz and 480 Hz, from the ISO 200 video (blue) and the ISO12800 video (red), and (b) PSDs from the respective signals and from some other ISO values in-between. ....	38
Figure 14: Single shaker 100Hz test setup. (a) Camera and Shaker and (b) Cropped grey scale video frame. ....	40

Figure 15: $7.5 \times 10^{-2}$ mm RMS (a) time domain signal (red) with background noise (blue) and (b) Respective PSDs. $2.3 \times 10^{-4}$ mm RMS (c) time domain signal (red) with background noise (blue) and (d) Respective PSDs. ....	41
Figure 16: Pink noise experiment setup .....	42
Figure 17: Pink noise experiment results: (a) PSDs of the first (red) and second (blue) shaker regions and of the background noise (grey) with the bandwidth selected for the correlation coefficients calculation is shaded in grey, (b) Coherence between shaker regions (black) (c) CPSD between the shaker regions (black), (d) Unwrapped phase between shaker regions (black) and a zero degree phase line (green) for comparison, (e) Autocorrelation Coefficient of the first and second shaker regions and the Cross Correlation Coefficient between regions.....	43
Figure 18: Test Bench: a) Schematic of the pipe response due to leak noise excitation conducted by using the test bench; b) Test setup, c) Actuators (shakers) and sensors of the test bench.....	44
Figure 19: Schematic diagram for the wave propagation in a buried pipe system.....	45
Figure 20: Simulated conditions synthetic using the model (black solid line) and the actuator response measured by accelerometers (grey solid line) together with the background noise (blue dotted line). (a) PSD of P1; (b) PSD of P2; (c) Coherence between P1 and P2; (d) Modulus of the CPSD between P1 and P2; (e) Phase of the CPSD; (f) Correlation coefficient between P1 and P2. The frequency bandwidth over which the Cross-correlation coefficient is conducted is depicted in the phase.....	48
Figure 21: Experiment setup with the camera recording the test bench's shakers.....	49
Figure 22: (a) PSDs from the shaker 1 extracted by the camera (red) and accelerometer (yellow), from shaker 2 extracted by the camera (blue) and accelerometer (green), and the camera's background noise (dotted black). (b) CPSDs of the camera signals (black) and accelerometers' (grey). (c) Coherence of the camera signals and accelerometers'. (d) Unwrapped phase between camera signals and accelerometers'. (e) Cross Correlation Coefficient of the camera signals and accelerometers'.....	50
Figure 23: Distance experiment setup. ....	51
Figure 24: Distance experiment results. (a) PSDs from first shaker recorded at 50cm (red), at 150cm (blue), respective background noises (pink and light blue), and from the accelerometer (black), with the useful bandwidth delimited shaded grey, (b) The coherences between shakers signals at 50cm, 150cm, and accelerometer , (c) CPSDs between shakers signals at 50cm,	

150cm, and accelerometer, (d) Unwrapped phase between shaker signals at 50cm, 150cm, and accelerometer, (e) Cross Correlation Coefficient from the shaker signals at 50cm, 150cm, and accelerometer..... 52

Figure 25: Section of the videos' frames. (a) Sony RX100 IV and (b) Basler ace 2 a2A1920-160umBAS ..... 53

Figure 26: Results from the camera comparison, (a) PSDs from the shaker signals recorded with the Basler camera (red), with the Sony camera (blue), respective background noises (pink and light blue), and from the accelerometer (black) with the useful bandwidth for each camera delimited. (b) The coherences between shaker signals recorded with the Basler camera, with the Sony camera, and accelerometer (c) CPSDs from the shaker signals recorded with the Basler camera, with the Sony camera, respective background noises, and from the accelerometer. (d)Unwrapped phase between shaker signals recorded with the Basler camera, with the Sony camera, and accelerometer, (e) Cross Correlation Coefficient from the shaker signals recorded with the Basler camera, with the Sony camera and accelerometer. .... 54

Figure 27: Number of points being tracked. .... 55

Figure 28: Results from the number of points test. (a) PSDs from the displacement signals using 1 (blue) and 40 tracked points (red), with 10 and 20 intermediaries represented in grey. (b) Coherence between signals using 1 and 40 tracked points, with 10 and 20 intermediaries represented in grey..... 55

Figure 29: Different Pixel Kernel sizes..... 56

Figure 30: Different tracking areas and the reflection on the borders. .... 57

Figure 31: Time signal extracted from the camera using 11 pixels (red) and 201 pixels (blue) tracking neighborhoods..... 57

Figure 32: (a) PSDs of the signal extracted with different pixel neighborhoods: 11px (red), 201px (blue) and the accelerometer (black). (b) Coherence between signals extracted from the different shakers using different pixels neighborhoods and accelerometer. (c) CPSDs between the recorded signals of the shakers using different pixel neighborhoods and accelerometer. (d) Unwrapped phase between signals extracted from the different shakers using different pixels neighborhoods and accelerometer. (e) Cross Correlation Coefficients of the signals extracted from the different shakers using different pixels neighborhoods and accelerometer..... 58

Figure 33: Flowchart demonstrating the setup and application of the camera technique for vibration analysis. With the yellow representing the object preparation, blue the camera setup, red the recording stage, and green the pos-processing. .... 61

Figure 34: Experiment schematic. .... 63

Figure 35: Results of the experiment using the leak noise simulator test bench: (a) PSDs from the first shaker extracted with the camera (red) and accelerometer (yellow), and from the second shaker extracted with the camera (dark blue) and accelerometer (light blue). The background noise is also depicted for the camera (dotted grey) and accelerometer (dotted orange). The shaded regions represent the useful bandwidth. (b) The Coherence between camera signals (black), and accelerometer signals (grey). (c) The CPSDs from the camera signals and accelerometer signals. (d) The Unwrapped phase between camera signals, accelerometer signals and the theoretical phase (dashed green line). (e) The Cross Correlation Coefficient presenting the time delay performed using camera signals and accelerometer signals..... 64

Figure 36: (a) Leak location found by the water company. (b) Distribution of tracked points and accelerometers. .... 65

Figure 37: Camera video frame, highlighting one the ground mark used to facilitate the tracking procedure using camera. .... 66

Figure 38: Camera Experiment Setup. (a) Overview of the location with company technicians and engineers, (b) Camera and Acquisition system assembly, (c) Accelerometer positions, (d) camera recording position for the line recording. .... 66

Figure 39: Water leak fixing process: (a) Dug hole, (b) Exposed pipes and water being pumped, (c) Real leak position representation, (d) Leak fixed with a repair clamp. .... 67

Figure 40: PSDs of the signals from accelerometers 1 (blue dashed line) and 3 (red dashed line) together with extracted signals with the camera (grey scale) at these positions..... 68

Figure 41: Correlation of camera data: (a) Unwrapped Phase (b) Coherence and (c) Cross Correlation Coefficient. The labels “i”, “ii”, “iii” and “iv” are the analysis between points 3 and 1; 3 and 2; 3 and 4; and 3 and 5, respectively. The dashed lines on the phase plots are the theoretical phases calculated using the delay given by the Cross correlation coefficient. .... 69

Figure 42: Correlation of Accelerometer “1” and “3” data: (a) Unwrapped Phase, (b) Coherence, (c) Cross Correlation Coefficient from accelerometer data. .... 70

Figure 43: Photo of the unburied pipe experiment setup..... 80

Figure 44: PSDs from the camera signal on the leak (red), its background noise (green), from the accelerometer on the leak (blue), and its background noise (yellow) ..... 81

Figure 45: (a) PSDs from the Leak position (black), 1m (red), 2m (green) and 3m (blue), along with the background noise (dashed black). (b) Coherence plot between the leak and three different distance points. .... 81

**LIST OF TABLES**

Table 1: Parameter values used on the test bench for leak simulation.....47

## LIST OF ABBREVIATIONS AND ACRONYMS

CAMshift	Continuously Adaptive Meanshift
CPSD	Cross Power Spectral Density
DIC	Digital Image Correlation
FRF	Frequency Response functions
GPR	Ground Penetrating Radar
ISO	International Organization for Standardization
PSD	Power Spectral Density
PVC	Polyvinyl chloride
RAM	Random Access Memory
RMS	Root Mean Square
SNR	Signal-to-Noise Ratio
UK	United Kingdom

## LIST OF SYMBOLS

$A$	Matrix of intensities spatial gradients in $x$ and $y$ directions for all pixel in the tracking neighborhood.
$a_c(t)$	Time signal of a pipe wall acceleration due to a leak. [m/s <sup>2</sup> ]
$\vec{b}$	Vector of intensities time gradients for all pixel in the tracking neighborhood.
$c$	Wave speed. [m/s]
$C_{x_1x_2}(f)$	Coherence function between signals at frequency $f$ .
$d$	Distance between sensors 1 and 2. [m]
$d_c$	Distance between camera and object of interest. [m]
$d_1, d_2$	Distance between leak and sensors 1 and 2, respectively. [m]
$E$	Expectation or Ensemble average function
$f$	Frequency. [Hz]
$f_x$	Pixel intensity spatial gradient in the $x$ direction [1/pixel].
$f_y$	Pixel intensity spatial gradient in the $y$ direction [1/pixel].
$f_t$	Pixel intensity time gradient[1/s].
$\theta$	Angle between camera and object surface. (°)
$I_{x,y}$	Pixel intensity calculated by the Sobel operator representing the intensity gradient in $x$ and/or $y$ direction.
$I$	Pixel intensity value.
$k$	Wave number. [rad/m]
$\lambda_1, \lambda_2$	Eigenvalues of the $M$ matrix.
$L$	Leak Spectrum function.
$M$	Edge detectors structural tensor.

$N$	Number of pixels in the neighborhood.
$\rho(\tau)$	Cross-correlation coefficient at the time delay between signals $\tau$ .
$R_{x_1x_2}(\tau)$	Cross-correlation function at the time delay between signals $\tau$ .
$R$	Harris Edge Detector score function.
$r$	Sensitivity parameter for Edge/Corner detection methods.
$S_{xx}(f)$	Power Spectral Density of the displacement time signal $x(t)$ . [ $\text{m}^2/\text{Hz}$ ]
$S_{x_1x_2}(f)$	Cross Power Spectral Density (CPSD) function between the displacement time signals $x_1(t)$ and $x_2(t)$ . [ $\text{m}^2/\text{Hz}$ ]
$T$	Time interval of the signal. [s]
$t$	Time [s].
$\tau$	Time delay between signals. [s]
$u$	Velocity in video in the $x$ direction [pixels/s].
$v$	Velocity in video in the $y$ direction [pixels/s].
$\phi(f)$	Phase function between two signals at frequency $f$ . [rad]
$W$	Window function that gives more influence to constraints at the center of the neighborhood.
$W_d$	Diagonal matrix composed by $W(x_i, y_i)$ , where $i=1,2,\dots,N$ .
$x$	Position in the horizontal direction [pixels].
$X(f)$	Finite Fourier transform of the time signal $x(t)$ .
$y$	Position in the vertical direction [pixels].
$\omega$	Frequency. [rad/s]

## TABLE OF CONTENTS

<b>CHAPTER 1: THEORETICAL BACKGROUND.....</b>	<b>13</b>
1.1. Overview on leak detection and localization.....	13
1.2. Leak noise vibroacoustic sensors and techniques. ....	15
1.3. Techniques for leak detection using ground measurements.....	17
1.4. Computer vision applied to problems in engineering.....	18
1.5. Motivation .....	20
1.6. Objectives .....	20
1.7. Summary of dissertation.....	21
<b>CHAPTER 2: OVERVIEW ON CAMERA IMAGE AND SIGNAL PROCESSING FOR MECHANICAL SYSTEM RESPONSE MEASUREMENTS.....</b>	<b>22</b>
2.1. Object tracking .....	22
2.1.1. Optical Flow .....	24
2.1.2. Corner detection .....	26
2.1.3. Virtual video corner tracking.....	29
2.2. Classical signal processing .....	30
2.3. Chapter Summary .....	32
<b>CHAPTER 3: CAMERA TECHNIQUE CHARACTERIZATION .....</b>	<b>34</b>
3.1. Contrast Influence.....	34
3.2. Angle Influence .....	35
3.3. ISO Influence.....	37
3.4. Single Shaker Test.....	39
3.4.1. 100Hz Sine Signal .....	39
3.4.2. Pink Noise Signal .....	41
3.5. Leak Noise Simulator Test Bench.....	44
3.6. Random noise .....	49

3.7.	Distance Influence.....	51
3.8.	Camera Comparison.....	53
3.9.	Number of tracked points influence.....	55
3.10.	Pixel Neighborhood Size Influence .....	56
3.11.	Chapter Summary and Rule of thumb.....	59

**CHAPTER 4: INITIAL INVESTIGATION ON LEAK DETECTION USING CAMERAS 62**

4.1.	Simulated leak noise – pipe response .....	62
4.1.1.	Leak data collected in the UK.....	62
4.2.	Real Leak Experiment – ground vibration.....	65
4.2.1.	Trento leak test.....	65
4.3.	Chapter summary .....	71

**CHAPTER 5: CONCLUSION AND DISCUSSION ..... 72**

**REFERENCES ..... 74**

**APPENDIX A..... 80**

A.1 -	Tupã Test Rig Experiment.....	80
-------	-------------------------------	----

## **CHAPTER 1: THEORETICAL BACKGROUND**

This chapter introduces the fields of water leak detection, localization, and computer vision. It begins with an overview of methods and sensors for detecting leaks in underground pipes, examining their applications and limitations, and includes a detailed analysis of vibroacoustic techniques alongside ground surface measurements. It then explores the diverse applications of computer vision in modern engineering, focusing on motion-tracking techniques for structural and dynamic analysis. Based on these insights, the chapter defines the motivation and objectives of this study.

### **1.1. Overview on leak detection and localization**

When water is conveyed from treatment facilities to end consumers, a significant portion is wasted within water distribution networks. Non-Revenue Water (NRW) is a critical issue, particularly in developing countries. For example, in Brazil, up to 38% of the total potable water supply is lost before it even reaches households and buildings [1]. In some places, this percentage can exceed 70%.

Different leak detection methods and devices are employed depending on the specific situation. For large areas and particularly wide water mains, strategically placed sensors that monitor water pressure and flow rate can provide an initial indication of potential leak zones. This preliminary assessment helps narrow down the areas where leaks can be located, enabling more precise location techniques with specialized tools to pinpoint their position. One such method is thermal imaging, which employs handheld thermal cameras or drones to scan the ground surface above buried pipes. This is conducted by detecting abnormal temperature variations, leaks can be identified [2]. Bach and Kodikara [3] evaluated the use of infrared cameras for thermal measurements to localize leaks and demonstrated their potential as an over-ground leak localization technique. However their findings also highlighted significant limitations: the method detected only 59% of leaks and faced challenges related to surface thermal and hydraulic properties, seasonal factors, viewing angles, and distance. Yahia, et al. [4] expanded on the infrared camera technique by analyzing the time variance of the thermal profile over the leak region. Conducting some averaging and image processing, they showed it is possible to reduce false positives and achieve better accuracy in locating leaks. However, this

approach typically requires monitoring the region of interest for several hours or at different times during the day, making it a time-consuming method compared to traditional techniques.

Acoustic techniques, particularly simple analog listening sticks and single-sensor digital versions, are widely used for leak detection due to their affordability and portability [5]. However, for higher precision in pinpoint leak location, more advanced methods are often required. Usually, the leak detection process begins with listening devices, such as the listening sticks for pipes and geophones for the ground surfaces. Listening sticks are acoustic tools designed to detect vibrations caused by leaks. They consist of a metal rod connected to either a diaphragm with a resonance chamber or a digital display. When placed directly on a pipe or the ground above a buried pipe, these devices amplify vibrations traveling along the rod, allowing the user to hear leak noises more distinctly. It is important to note that effectively using basic listening sticks and geophones requires user training and experience to correctly interpret the sounds and locate leaks accurately [2,5].

For more precise measurements, complex systems can be used. Khulief et al. [6] used a moving hydrophone to measure acoustic pressure inside a test rig's pipe. The sensor's location is tracked by a set of transponders and the leak is located based on variation in the acoustic frequency response at different positions within the pipe. Acoustic loggers, on the other hand, are devices that measure the acoustic emission or vibration in pipe branches over extended periods. By correlating data from multiple loggers, specific software can detect and potentially locate leaks in large water pipes networks. Xue, et al. [7] used many acoustic loggers to locate water leaks in Suzhou, China. They compared the method to manual detection methods, and analyzed the critical parameters of the logger system required to ensure reliable results.

Ground Penetrating Radar (GPR) is a nondestructive testing technique that uses high-frequency electromagnetic pulses to transmit and receive reflected echoes. This allows for the detection of gaps or changes in material properties within the soil caused by leaking water around buried pipes, thereby identifying leaks in water distribution systems [8]. GPR is particularly effective with PVC pipes but faces challenges when dealing with metal pipes. Metals act as strong reflectors of the waves, preventing the signal from passing through. Moreover, due to high electrical conductivity of metal, radar energy is rapidly attenuated, resulting in reduced penetration depths and significantly diminishing GPR's effectiveness [9].

Leak noise correlators are advanced acoustic devices designed for pinpointing the leak location. These devices operated by simultaneously measuring vibration or sound pressure signals at two points surrounding the suspected leak using two sensors. By applying cross correlation to these signals, the time delay between them can be estimated. This time delay is

then used to estimate the distance from one of the sensors to the actual leak position [5]. Scussel, et al. [10] presented a series of measurements conducted in various test fields using the noise correlation system and provided a detailed discussion of the key variables that affect the results.

While noise correlator techniques are more precise compared to other methods, they usually require direct access to the pipe for sensor placement. This can pose challenges, particularly for pipes buried at significant depths. Therefore, it may be necessary to either excavate down to the pipe or include dedicated access points during the pipeline's design and construction phases. In order to minimize disruption to roads and sidewalks, and avoid unnecessary excavation, non-contact techniques have gained significant attention in recent years. Examples include infrared sensors in thermal methods and Ground Penetrating Radar (GPR)[8] (as previously described). The intention of this work is to contribute to the advancement of leak detection in buried pipes exploring the use of non-contact sensors, more specifically camera measurements, something not yet explored, combined with vibro-acoustic techniques similar to the ones employed in leak noise correlators. Traditional commercial video cameras have already been used in different dynamic analysis applications, showing promising results for its application on the ground vibration measurements intended [11,12].

## 1.2. Leak noise vibroacoustic sensors and techniques.

- **Listening sticks:** These are tools that are used to detect leaks that are occurring in the ground or in subterranean pipes. To transmit the vibration to an electro-mechanical transducer that digitally amplifies the leak sound in electronic listening sticks or to a membrane within a resonant cavity that amplifies the leak sound in mechanical listening sticks the stick is made of a rigid material, like steel or wood. Operators often begin the listening stick leak localization process by examining a pipe network for leaks by listening to the sound at many access points. When operators come across a suspected leak, they locate it by listening at short intervals of around one meter on the ground directly above the pipe [13,14].
- **Hydrophones:** Similar to how microphones are made to hear sound in the air, hydrophones are sensors made to hear sound in the water. Hydrophones are typically piezoelectric transducers with a sensing element that produces an electrical potential in response to a change in the water's acoustic pressure [15].

The purpose of these devices is to detect leaks by inserting them into pipes at easily accessible locations, such as manholes or hydrants [13].

- **Geophones:** These are sensors made to quantify motion in terms of velocity or displacement. They are made up of a moving mass wrapped in a wire coil and hung over a magnet by a spring. An electrical signal expressed in terms of voltage is produced when the mass moves because of the interaction between the movement and the magnetic field, which causes an electrical current to flow through the wire coil [16]. Certain geophone-based devices are made to function as microphones. An electro-mechanical transducer converts sound produced by the device's resonant chamber, which is placed on a rigid plate on the ground, into voltage [13].
- **Accelerometer:** Accelerometers are devices that measure acceleration forces. They are used in water leak detection on underground pipes by converting mechanical motion, such as vibrations caused by leaks, into electrical signals. When an accelerometer is subjected to acceleration, it generates a voltage proportional to the acceleration, usually through the implementation of piezoelectric materials. This voltage can then be measured and used to determine the acceleration experienced by the accelerometer [17].
- **Leak Noise Correlators:** Computer-based tools that are used to locate leaks along a straight section of a pipeline. The localization process is often based on synchronized measurements of leak sound using hydrophones or pipe-wall vibration applying accelerometers at two separate locations along a straight stretch where the leak could be situated. Cross-correlation is then used to determine the time delay between the two signals. The leak position relative to one of the sensors is determined by integrating the time delay, the leak noise velocity in the pipe, and the distance between the two sensors [13,14,18,19].

Leak noise correlators' major advantage is that, before computing cross-correlation, the signals can be immediately processed through a bandpass filter in the computer-based equipment [14,18]. When the cut-off frequencies for the bandpass filter are appropriately chosen, this process makes such devices highly resilient to uncorrelated noise, since the associated SNR is improved [20]. Because of its simplicity and efficacy in comparison to other leak localization techniques, leak noise correlators have historically been one of the most often used devices on leak surveys [18]. The primary drawback of leak noise correlators

is that the method for estimating the leak position depends on knowing the velocity at which leak noise propagates through the pipe. Values for such a velocity are often computed empirically for various pipe diameters, pipe materials, and sensor types and stored in leak noise correlators [21]. However, there is a great variability among them [22]. As one possible solution, the velocity of leak noise propagation can be measured in-situ by strongly exciting the pipe using an actuator and measuring the interval that it takes to travel a specific piece of the pipe between two sensors [23].

### **1.3. Techniques for leak detection using ground measurements.**

In addition to producing sound waves that travel through the buried pipe, a leak also emits waves directly into the soil, detectable on the surface [24]. Though understanding leak noise generation remains complex, Burn et al. [25] categorized it into three source types based on where acoustic waves form. The first type originates from water flowing through the leak orifice, interacting with the pipe wall to create waves along the buried pipe. The second type arises from the water jet's impact with the underground cavity wall, and the third stems from water circulating inside the underground cavity; both generate waves that spread into the soil. However, these waves weaken significantly with distance, limiting leak localization methods using ground surface vibration measurements to relatively close positions. One of the main techniques for ground measurement leak detection is the Passive Seismic Wave Technique.

Wang et al. [26] proposed passive seismic wave approaches, which are a leak localization strategy. This approach yields leak coordinates in two dimensions, while Cheng et al. [27] expanded it to three dimensions. Both approaches use concepts of compressional and shear wave measurements techniques, but they do not use an excitation mechanism to generate soil waves, as used in techniques to detect the pipe itself. Instead, a leak in the buried pipe causes acoustic waves to propagate through the soil and be detected at the ground surface by a network of inline sensors. The time gap between sensor pairs along a pipeline is computed by considering the expected wave speed in the soil as well as the relative distance the wave travels from the leak to a surface sensor, which might be in two or three dimensions. After measuring the ground surface vibrations, the temporal differences between sensor pairs are evaluated using a cross-correlation function. These time differences are then used in an optimization algorithm to estimate the leak's position in either two or three dimensions.

The convenience of not needing any kind of excitation equipment to create acoustic waves in the soil, as well as the ability to reach subterranean pipes without difficulty, are the primary benefits of passive seismic wave approaches. However, the primary drawback of passive seismic methods is that they need to estimate the speed of waves in the soil in order to compute the difference in time between two ground-surface sensors' measurements of ground vibration [26,27]. This can be highly problematic since multiple wave types can propagate in the soil, and as the soil may not be homogeneous, the corresponding wave speed may vary for different regions.

#### **1.4. Computer vision applied to problems in engineering.**

Computer vision is a combination of image processing, pattern recognition, and data extraction. A mechanism aimed at analyzing, modifying, and providing a high-level understanding of images, its purpose is determining what is occurring in the captured images, use this to determine the command to be sent to a computer or electronic controller, or to provide another image with additional information in relation to the analyzed [28, 29].

The steps involved in image analysis include, first Image Creation, which involves capturing and storing an object's image. Then Image Processing, aiming to enhance image quality and detail through contrast, color, and resolution manipulation, for example. Next, the Image Segmentation, where the object of interest is determined and separated from the background information. The fourth stage is Image Measurement, involving the quantization of various significant features, like object position, size, shape, and even distance; and last the Image Interpretation, where the extracted images are then interpreted, in this last stage deep learning or artificial intelligence algorithms can be applied to provide better or faster results [28,30]. This technology aids in evaluating an athlete's performance, assists medical professionals in identifying illnesses, contributes to meteorological forecasting by calculating cloud movements, and is even utilized in determining structural deformations and displacements [31,32].

In the field engineering, cameras are being used to measure the dynamics of structures where the access is limited or impractical or the object is big enough to demand too many sensors for a single measurement. Chen et al. [33] analyzed the vibration of an antenna on a high tower using a camera 175m away and shows the possibilities to use this sensor for structural health monitoring. The use of cameras for evaluation of bridge deformations and vibrations is extensive. Ghyabi et al. [34] showed the advantages and limitations of the

application of different camera-based techniques to measure two bridges deflections comparing to traditional string potentiometers. Feng and Feng [35] used one camera for calculating the natural frequencies and mode shapes of the Manhattan bridge by measuring 30 points along the structure. Ojio et al. [36] used cameras to calculate the deflection of a bridge, which structural parameters are already known, and then estimate the weight of vehicles passing over it.

The dynamics of structural cables are extremely hard to measure with traditional contact sensors like accelerometers and piezoelectric strain sensors, either due to the difficulty to access these parts, the number of sensors and preparation time needed, or even the interference of the sensors on the structure itself [37,38]. Many techniques are being developed using video cameras to determine the tension on suspension bridges' cables. Wang et al. [39] used a smartphone to record different markers over a bridge structure and cables and, through the video processing, can calculate the natural frequencies and cable tension. Wangchuk et al. [40] used video magnification and feature tracking techniques applied to recordings of bridge cables to extract their modal parameters and the cables' tensions. Wang et al. [41] and Zang et al. [42] enhanced the quality of camera techniques for bridge cables measurements in complex situations, including the use of cameras mounted on drones.

Camera techniques are being used to perform detailed modal analysis and dynamic monitoring of complex structures with in-situ measurements. Khadka et al. [43] developed a technique for extraction of vibration characteristics and deflection shapes of wind turbines using a Digital Image Correlation (DIC) system mounted on a drone, allowing the monitoring of these structures during operation. Čufar, Slavič, and Boltežar [44] developed a hybrid technique of video magnification for modal shapes extraction using some modal parameters extracted with accelerometers, the method is tested on a long beam and then applied to the analysis of a complex impeller cover. Egner et al. [45] performed a modal analysis of a car coil spring using a stereo camera setup for 3D measurements and compares the results with an experimental modal analysis using accelerometers. Krivic, and Slavič [46] used a video camera along with a laser vibrometer and a thermal camera to perform the calculation of temperature-dependent material properties, like damping, elastic modulus, and coefficient of thermal expansion, of composite 3D printed samples. Bregar, et al. [47] developed a technique that combines camera measurements and accelerometer data of a structure to produce better quality FRFs. The full-field displacement is extracted with the camera, the complex eigenvalues are identified from the accelerometer data, and, with a hybrid model, mode shapes are identified and the FRFs are reconstructed.

Most modern image-based techniques for vibration analysis combine the camera measurements with an extra sensor, like an accelerometer or laser vibrometer, to generate better results. In this project, the intention was to extract the best of the camera measurements alone applied to leak detection and ground vibration measurements, something never tried, yet. Therefore, multiple experiments were applied to verify the influence of different variables on the camera results and then provide better results focusing on water leak detection through the control of these parameters and signal processing. The extra sensors were used just for comparison and validation of the camera results.

## **1.5. Motivation**

The proposed work aims to address part of the research gap in the use of non-contact measures together with vibro-acoustic techniques for leak detection in buried pipes. Non-contact measures provide advantages, particularly in accessing challenging measurement positions where traditional contact sensors face limitations due to coupling requirements. Here the attempt is to use ordinary cameras together with computer vision techniques to extract meaningful motion of surfaces. Moreover, ordinary cameras offer easier accessibility and potentially lower costs compared to high-sensitivity accelerometers or laser vibrometers, making them a practical alternative. Therefore, it is important to understand the limitations of using ordinary cameras as non-contact sensors for this application, verify the advantages, and identify the key variables that with to generate the best results.

## **1.6. Objectives**

The main objectives of this work are as follow:

- Develop a technique applied to traditional video cameras using computer vision and non-contact sensing methods to detect and extract surface displacement presenting low vibration levels, with the goal of locating water leaks in buried pipelines.
- Investigate the influence of different camera parameters to establish a guideline for operating the new developed technique and achieving representative results for the leak detection field.

## **1.7. Summary of dissertation**

Chapter 1 herein described highlights the techniques, sensors and signal processing methods commonly used in leak detection, along with the study's motivation and the objectives. Chapter 2 delves into the basis of the camera tracking process and classical signal processing tools used to characterize the pipe system's response due to a leak excitation. Chapter 3 covers the steps and experiments conducted to establish a procedure for setting up the camera aiming at a low Signal-to-Noise Ratio (SNR) measurements focused on extracting meaningful vibration data caused by leaks. Chapter 4 presents the mains results obtained using the proposed image extraction procedures together with classical signals processing tools. These results were achieved via using a specific bespoke test bench where controlled leak situations can be simulated as a proof of concept. Besides, actual leak detection using ground vibration was also carried out, yielding promising results for using cameras as a non-contact measurement to locate leaks. Finally, Chapter 5 summarizes the main conclusions and outlines potential directions for future work.

## CHAPTER 5: CONCLUSION AND DISCUSSION

This project focused on developing a computer vision technique to track point displacements, alongside methods for vibration analysis and signal processing for detecting water leaks in buried pipes. An comprehensive analysis was conducted to evaluate the influence of key variables on displacement signals extracted from videos recordings using sparse Optical Flow tracking and corner detection techniques. As a result, a guideline (or rule of thumb) was established to identify the best parameter set for achieving better signal definition and minimizing background noise. These parameters can be summarized as:

- High contrast and edge definition between the tracked object and its background.
- Low camera angles relative to the object's surface to minimize distortion.
- Low ISO sensitivity, provided that it maintains good object visibility and contrast.
- Close proximity between the camera and the object, as shorter distances improve precision.
- A high density of tracking within the small area being analyzed.
- A relatively large Lucas-Kanade Optical Flow pixel neighborhood.
- Video duration of 30 up to 60 seconds for optimal tracking performance.

These findings provide a systematic approach for improving the effectiveness of video-based displacement tracking techniques in leak detection applications.

After establishing an effective procedure to obtain low Signal-to-Noise Ratio (SNR) data, tests were conducted to evaluate the feasibility of the proposed technique for leak localization. The first experiment, conducted on a bespoke test bench called the Leak Noise Simulator, demonstrated the method's capability to use a single camera to extract displacement signals from different areas simultaneously. By correlating these signals and estimating time delays, the camera successfully determined the simulated leak's position with high accuracy. This experiment highlighted the technique's potential under controlled conditions, validating its effectiveness for detecting and locating leaks.

The second experiment was conducted in a real-world setting in downtown Trento (Italy), where ground vibrations near an actual leak were measured. This test presented additional challenges, including urban noise and a frequency content of the leak energy that often

exceeded the Nyquist frequency of the camera. Despite these limitations, the camera managed to extract ground displacement signals within a narrow low-frequency bandwidth and calculated proportional time delays between points on the ground, indicating the direction of the leak source. However, the accelerometer data revealed that the calculated delays were not accurate, likely due to time aliasing.

Although the results of the second experiment were less precise, they do not undermine the potential of the proposed method. On the contrary, they demonstrate the promise of combining non-contact measurement techniques with classic signal processing methods for leak localization. The findings suggest that with improved setups or conditions, the camera-based approach could be a potential tool for detecting and locating leaks in water systems even via measuring ground vibration.

The experiments revealed that commercial cameras face some drawbacks for vibration analysis, primarily the background noise level and sampling rate limitations. While the developed procedure significantly reduced background noise, it remains higher than that of traditional sensors like high-sensitive piezoelectric accelerometers, which are commonly used in leak detection surveys. Additionally, the cameras' sampling rates, which under specific conditions can reach only a few kilohertz, restrict the analysis to low-frequency content.

Despite these limitations, the camera technique demonstrated promising initial results in leak localization through non-contact measurements, offering a relatively lower-cost alternative to more expensive sensors like laser vibrometers and ground-penetrating radar (GPR). Future improvements could involve employing high-resolution cameras or synchronizing multiple cameras to monitor different sections of a pipeline. Additionally, enhancements in signal processing, such as the application of array signal processing techniques, could also help refine the approach and more accurately identify the direction of the noise source.

## REFERENCES

- [1] Ribeiro, A.P., (2018). “O Século da Escassez”. O Globo (Printed Issue 24/03/2018, p.8).
- [2] Kilinski, M.A., “Overview of Leak Detection Technologies A Summary of Capabilities and Costs”. Pacific Northwest National Lab Report, PNNL-28885, 2019.
- [3] Bach, P. M., and Kodikara, J. K. (2017). Reliability of Infrared Thermography in Detecting Leaks in Buried Water Reticulation Pipes. *IEEE Journal of Selected Topics in Applied Earth Observations and Remote Sensing*, 10(9), 4210–4224.
- [4] Yahia, M., et al. (2021). Non-Destructive Water Leak Detection Using Multitemporal Infrared Thermography. *IEEE Access*, 9, 72556-72567.
- [5] O. Hunaidi, et al. Detecting leaks in plastic pipes. *Journal-American Water Works Association*, 92(2), 82-94, 2000.
- [6] Khulief, Y., et al. (2012). Acoustic Detection of Leaks in Water Pipelines Using Measurements inside Pipe. *Journal of Pipeline Systems Engineering and Practice*, 3, 47-54.
- [7] Xue, Z., et al. (2020). Application of acoustic intelligent leak detection in an urban water supply pipe network. *Journal of Water Supply: Research and Technology-Aqua*.
- [8] N.A.M. Yussof, and H.W. Ho. “Review of Water Leak Detection Methods in Smart Building Applications”. *Buildings*, 12(10), 1535, 2022.
- [9] Amran, T. S. T., et al. (2019). “A study on detection water leakage of underground metal and PVC pipes using ground penetrating radar”. In *IOP Conference Series: Materials Science and Engineering* (Vol. 555, No. 1, p. 012012). IOP Publishing.
- [10] Scussel, O., et al. (2023). “Key Factors That Influence the Frequency Range of Measured Leak Noise in Buried Plastic Water Pipes: Theory and Experiment”. In *Acoustics* (Vol. 5, No. 2, pp. 490-508). MDPI.
- [11] J. Javh, J. Slavič, and M. Boltežar. “Experimental modal analysis on full-field DSLR camera footage using spectral Optical Flow imaging”. *Journal of Sound and Vibration*, 434, 213-220, 2018.
- [12] L. Praticò, et al. “Experimental and numerical vibration analysis of plates with curvilinear sub-stiffeners”. *Engineering Structures*, 209, 109956, 2020.
- [13] Iwanaga, M.K. (2023). “Investigation of ground surface vibration to locate leaks in buried water pipes”, PhD teses, UNESP- Faculdade de Engenharia- Ilha Solteira-SP
- [14] Hunaidi, O. (2000). “Detecting leaks in water-distribution pipes”. Ottawa: Institute for Research in Construction, National Research Council of Canada.
- [15] Azo Sensors. What is a hydrophone? 2012. Available in: <<https://www.azosensors.com/article.aspx?ArticleID=13>>. Accessed on: 3 May. 2024.

- [16] Earth Sciences. (2021). “The geophone: how we listen to the Earth”. Available in: <<https://www.esearth.com/the-geophone-how-we-listen-to-the-earth/>>. Accessed on: 3 May. 2024.
- [17] McMillen, C. (2021) “Accelerometers: How do they Work?”, Baker Hughe Article, Available in: <<https://www.bakerhughes.com/bently-nevada/orbit-home/orbit-article/accelerometers-how-do-they-work>> Accessed on: 3 May. 2024.
- [18] Fuchs, H.V., Riehle, R. (1991) “Ten years of experience with leak detection by acoustic signal analysis”. *Applied Acoustics*, Oxford, v. 33, n. 1, p. 1-19.
- [19] Glentis, G. O., Angelopoulos, K., (2019). “Leakage detection using leak noise correlation techniques – Overview and implementation aspects”. PAN-HELLENIC CONFERENCE ON INFORMATICS, 23., Nicosia. Proceedings of the 23rd Pan-Hellenic Conference on Informatics. New York: Association for Computing Machinery 2019, p. 50-57.
- [20] Gao Y, Brennan M J, Muggleton J M and Hunaidi, O (2004), “A model of the correlation function of leak noise in buried plastic pipes”, *Journal of Sound and Vibration*, Vol. 277, pp. 133-148.
- [21] ADS. (2010) “Eureka2R leak noise correlator user manual”. Available in: <https://www.adsenv.com/sites/default/files/manuals/adseureka2rusermanuala1.pdf>. Accessed on: 3 May. 2024.
- [22] Sewerin. (2023). “Leak detection in water distribution networks by correlation sound velocity as a possible source of error”. Available in: <https://www.sewerin.com/us/info-center/publications/leak-detection-in-drinking-water-distribution-networks>. Accessed on: 3 May. 2024.
- [23] Almeida, F. C. L., Brennan, M. J., Lima, F. K., Iwanaga, M. K., Scussel, O. (2021). “Using a geophone as an actuator to estimate the velocity of leak noise propagation in buried water pipes”. *Applied Acoustics*, Oxford, v. 184, n. 108251.
- [24] Zhang, P, et al. (2022). “Ground vibration analysis of leak signals from buried liquid-filled pipes: An experimental investigation”. *Applied Acoustics*, Oxford, v. 200.
- [25] Burn, S., et al. (1999) “Pipe leakage – Future challenges and solutions.”. Available in: <[https://www.researchgate.net/publication/44055423\\_Pipe\\_Leakage\\_-\\_Future\\_Challenges\\_and\\_Solutions](https://www.researchgate.net/publication/44055423_Pipe_Leakage_-_Future_Challenges_and_Solutions)>. Accessed on: 3 May. 2024.
- [26] Wang, J.; Liu, J.; Liu, H.; Tian, Z.; Cheng, F. (2017). “Modeling and locating underground water pipe leak with microseismic data”. *Journal of Applied Geophysics*, Amsterdam, v. 136, p. 1-8.
- [27] Cheng, F.; Liu, J.; Wang, J.; Yang, Z.; Abbasi, S. S.; Tian, Z.; Xu, H. (2018). “Locating leaking buried pipes based on ground microseismic records in 3D space”. *Surveys in Geophysics*, Dordrecht, v. 39, p. 993-1007.
- [28] Wiley, V., & Lucas, T. (2018). Computer vision and image processing: a paper review. *International Journal of Artificial Intelligence Research*, 2(1), 29-36.

- [29] Pulli, K., Baksheev, A., Korniyakov, K., & Eruhimov, V. (2012). Real-time computer vision with OpenCV. *Communications of the ACM*, 55(6), 61-69.
- [30] Mery, D., Pedreschi, F., & Soto, A. (2013). Automated design of a computer vision system for visual food quality evaluation. *Food and Bioprocess Technology*, 6, 2093-2108.
- [31] Xu, S., et al. (2021). "Computer vision techniques in construction: a critical review." *Archives of Computational Methods in Engineering* 28.5, 3383-3397.
- [32] Esteva, A., et al. (2021). "Deep learning-enabled medical computer vision." *NPJ digital medicine* 4.1, 1-9.
- [33] Chen, J. G., et al. (2017). "Video camera-based vibration measurement for civil infrastructure applications." *Journal of Infrastructure Systems* 23.3: B4016013.
- [34] Ghyabi, M., et al. (2023). "Vision-based measurements to quantify bridge deformations." *Journal of Bridge Engineering* 28.1: 05022010.
- [35] Feng, D., and Feng, M.Q., (2017). "Experimental validation of cost-effective vision-based structural health monitoring." *Mechanical Systems and Signal Processing* 88: 199-211.
- [36] Ojio, T., et al. (2016). "Contactless bridge weigh-in-motion." *Journal of Bridge Engineering* 21.7: 04016032.
- [37] Xu, Y., and Brownjohn, J.M.W., (2018). "Review of machine-vision based methodologies for displacement measurement in civil structures." *Journal of Civil Structural Health Monitoring* 8: 91-110.
- [38] Debasish, J., and Nagarajaiah, S. (2021). "Computer vision-based real-time cable tension estimation in Dubrovnik cable-stayed bridge using moving handheld video camera." *Structural Control and Health Monitoring* 28.5: e2713.
- [39] Wang, Yongwei, et al. (2021). "Research on non-contact and non-fixed cable force measurement based on smartphone." *Applied Sciences* 11.19: 8902.
- [40] Wangchuk, S., et al. (2022). "Modal analysis and tension estimation of stay cables using noncontact vision-based motion magnification method." *Structural Control and Health Monitoring* 29.7 : e2957.
- [41] Wang, Weidong, et al. (2023). "Target-free recognition of cable vibration in complex backgrounds based on computer vision." *Mechanical Systems and Signal Processing* 197: 110392.
- [42] Zang, Zongdi, et al. "Video-Based Vibration Measurement Using an Unmanned Aerial Vehicle: An Anti-Disturbance Algorithm for the Shaking of Airborne Cameras." *IEEE Transactions on Instrumentation and Measurement* (2023).
- [43] Khadka, A., et al. (2020). "Non-contact vibration monitoring of rotating wind turbines using a semi-autonomous UAV." *Mechanical Systems and Signal Processing* 138: 106446.
- [44] Čufar, K., Slavič, J., and Boltežar, M. (2024). "Mode-shape magnification in high-speed camera measurements". *Mechanical Systems and Signal Processing*, 213, 111336.

- [45] Egner, F. S., et al. (2022). High-speed camera based experimental modal analysis for dynamic testing of an automotive coil spring. *SAE International Journal of Advances and Current Practices in Mobility*, 4(1), 278-288.
- [46] Krivic, G., and Slavič, J. (2023). Simultaneous non-contact identification of the elastic modulus, damping and coefficient of thermal expansion in 3D-printed structures. *Polymer Testing*, 125, 108131.
- [47] Bregar, T., et al. (2021). Full-field FRF estimation from noisy high-speed-camera data using a dynamic substructuring approach. *Mechanical Systems and Signal Processing*, 150, 107263.
- [48] Soleimanitaleb, Z., Keyvanrad, M. A., and Jafari, A. (2019). "Object Tracking Methods: A Review". 2019 9th International Conference on Computer and Knowledge Engineering (ICCKE), (pp. 282-288), IEEE.
- [49] Thakore, D.G., Parekh ,H.S., and Udesang, K. J. (2014). "A survey on object detection and tracking methods". *International Journal of Innovative Research in Computer and Communication Engineering*, 2(2).
- [50] Fukunaga, K., and Hostetler, L.D. (1975). "The estimation of the gradient of a density function, with applications in pattern recognition". *IEEE Trans. Inf. Theory*, 21, 32-40.
- [51] Cheng, Y. (1995). "Mean Shift, Mode Seeking, and Clustering". *IEEE Trans. Pattern Anal. Mach. Intell.*, 17, 790-799.
- [52] Bradski, G. R. (1998). "Real time face and object tracking as a component of a perceptual user interface". In *Proceedings Fourth IEEE Workshop on Applications of Computer Vision. WACV'98 (Cat. No. 98EX201)* (pp. 214-219). IEEE.
- [53] Shen, C., Kim, J., & Wang, H. (2009). "Generalized kernel-based visual tracking". *IEEE Transactions on Circuits and Systems for Video Technology*, 20(1), 119-130.
- [54] Pan, B. (2011). "Recent progress in digital image correlation". *Experimental mechanics*, 51, 1223-1235.
- [55] Tissainayagam, P., & Suter, D. (2003). Contour tracking with automatic motion model switching. *Pattern Recognition*, 36(10), 2411–2427. doi:10.1016/s0031-3203(03)00088-8
- [56] Zeng, W., Zhu, G., & Li, Y. (2009). Point Matching Estimation for Moving Object Tracking Based on Kalman Filter. 2009 Eighth IEEE/ACIS International Conference on Computer and Information Science.
- [57] Beauchemin, S.S., and Barron, J.L., (1995) "The computation of Optical Flow." *ACM computing surveys (CSUR)* 27.3, 433-466.
- [58] Maciel, L.M.S., Maurílio, L., and Vieira, M.B., (2020) "Sparse Optical Flow Computation Using Wave Equation-Based Energy." *International Journal of Image and Graphics* 20.04, 2050027.
- [59] Fleet, D. and Weiss, Y. (2006). "Optical Flow estimation". In *Handbook of mathematical models in computer vision* (pp. 237-257). Boston, MA: Springer US.

- [60] Barron, J.L., Fleet, D.J., and Beauchemin, S.S., (1994) "Performance of Optical Flow techniques." *International journal of computer vision* 12.1, 43-77.
- [61] Fortun, D., Bouthemy, P., and Kervrann, C., (2015) "Optical Flow modeling and computation: A survey." *Computer Vision and Image Understanding*, 134, 1-21.
- [62] Lucas, B.D. and Kanade T. "An iterative image registration technique with an application to stereo vision". In *Proceedings of DARPA Image Understanding Workshop Vol. 81*, 121-130, 1981.
- [63] Liu, Y., et al. "A new methodology for pixel-quantitative precipitation nowcasting using a pyramid Lucas Kanade Optical Flow approach." *Journal of Hydrology* 529, 354-364, 2015.
- [64] Kitchen, L., and Rosenfeld, A. (1982). "Gray-level corner detection". *Pattern recognition letters*, 1(2), 95-102.
- [65] Sosa, J. C., Ortega, R., Garcia, V. H., Hernandez, R., and Ortega, N. Y. (2015). "Design and implementation of reconfigurable technology for edge detection in real time". 2015 IEEE Thirty Fifth Central American and Panama Convention (CONCAPAN XXXV).
- [66] Misra, S., & Wu, Y. (2019). "Machine learning assisted segmentation of scanning electron microscopy images of organic-rich shales with feature extraction and feature ranking". *Machine learning for subsurface characterization*, 289(3), 4.
- [67] Jähne, Bernd. "Digital image processing". Section 4 and 12, Springer Science & Business Media, 2005.
- [68] Harris, C., and Stephens, M. (1988). "A combined corner and edge detector". In *Alvey vision conference (Vol. 15, No. 50, pp. 10-5244)*.
- [69] Schmidt, A., Kraft, M., and Kasiński, A. (2010). "An evaluation of image feature detectors and descriptors for robot navigation". In *Computer Vision and Graphics: International Conference, ICCVG 2010, Warsaw, Poland, September 20-22, 2010, Proceedings, Part II (pp. 251-259)*. Springer Berlin Heidelberg.
- [70] Bansal, M., Kumar, M., and Kumar, K. (2021). "An efficient technique for object recognition using Shi-Tomasi corner detection algorithm". *Soft Computing*, 25, 4423-4432.
- [71] Sánchez, J., Monzón, N., & Salgado De La Nuez, A. (2018). "An analysis and implementation of the harris corner detector". *Image Processing On Line*.
- [72] Bendat, J.S., Piersol, A.G. (2010). "Random data: analysis and measurement procedures". 4th ed., John Wiley & Sons.
- [73] Welch, P. (1967). "The use of fast Fourier transform for the estimation of power spectra: A method based on time averaging over short, modified periodograms". *IEEE Transactions on audio and electroacoustics*, 15(2), 70-73.
- [74] Almeida, F., et al. (2014). "On the acoustic filtering of the pipe and sensor in a buried plastic water pipe and its effect on leak detection: an experimental investigation". *Sensors*, 14(3), 5595-5610.

- [75] M.K. Iwanaga, et al. "A laboratory-based leak noise simulator for buried water pipes". *Applied Acoustics*, 185, 108346. 2022.
- [76] Almeida F.C.L., Brennan M.J., Joseph P.F., Withfield S, Dray S and Pascoalini A.T. 2014. On the Acoustic Filtering of the Pipe and Sensor in a Buried Plastic Water Pipe and its Effect on Leak Detection: An Experimental Investigation. *Sensors (Basel)*, v. 14, p. 5595-5610.
- [77] Brennan, M.J., Karimi, M., Muggleton, J.M., Almeida, F.C.L., Lima, F.K., Ayala, P.C., Obata, D.H., Pascoalini, A.T. and Kessissoglou, N. 2018. On the effects of soil properties on leak noise propagation in plastic water distribution pipes. *Journal of Sound and Vibration*, Vol. 427, pp. 120 – 133.
- [78] Losson, Olivier, Ludovic Macaire, and Yanqin Yang. "Comparison of color demosaicing methods." *Advances in Imaging and electron Physics*. Vol. 162. Elsevier, 2010. 173-265.

## APPENDIX A

### A.1 - Tupã Test Rig Experiment

An experiment was performed in a test field in the city of Tupã. The objective was to analyze an unburied pipe response due to a leak and, by measuring different points, pinpoint the position of the leak. A first test was conducted recording the pipe response close to the leak and half a meter away from its position. Moreover, 2 accelerometers were positioned on the pipe wall over a section length covered by the camera. The accelerometer closer to the leak was protected from water drops via using a plastic bag. Checkerboard patterns stickers were also used to cover the pipe section of interest to enhance the camera tracking process. The photo of the setup used is shown in figure 43.

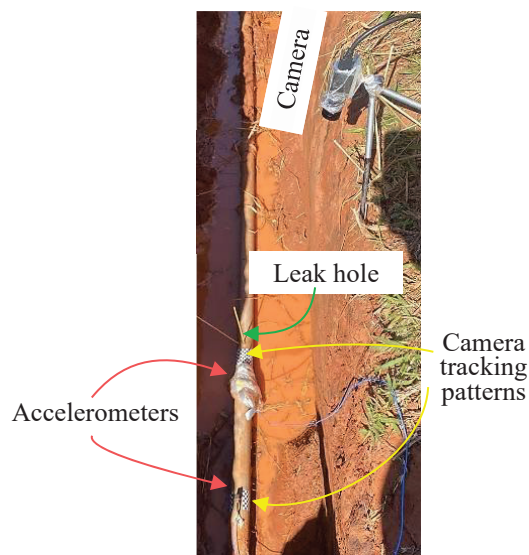


Figure 43: Photo of the unburied pipe experiment setup

The experiment started by conducting a measurement with the pipe pressurized with water. Air bubbles were removed by using a drainage valve located next to the end of the pipe section. Background measurements were also conducted for convenience. Moreover, the leak was induced by removing a wooden stick that blocked the hole. All the accelerometer data were converted to displacement for a better comparison with the camera results. The camera recorded at 1000 frames per second with a spatial resolution of 0.25mm/px. The PSDs can be visualized in figure 44.

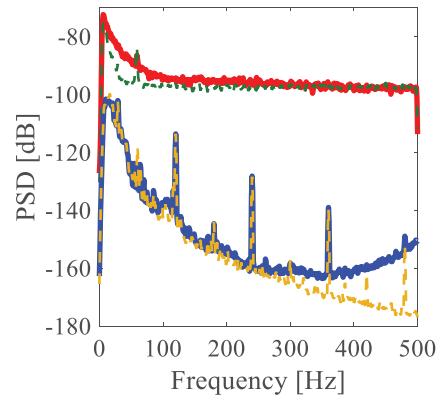


Figure 44: PSDs from the camera signal on the leak (red), its background noise (green), from the accelerometer on the leak (blue), and its background noise (yellow)

Figure 44 shows that the camera background noise is above the accelerometer leak signal within the frequency limit selected for the figure, which is in agreement with the frequency range that the camera presents a good response. Hence, the camera was not able to reach the level of the small displacements to capture the leak signal and, as the signal is attenuated with the distance along the pipe, the other recorded position presents even lower amplitudes to be captured. Another point to notice is that the accelerometer leak signal PSD practically matches its background noise until around 300 Hz, even the 60Hz harmonics generated by an electric transformer on a lamp post nearby. This indicates that, until 300Hz, the leak signal is lower even than the accelerometer limits. This is due to the hoop stiffness of the pipe that forces the response of the system to be located at frequencies higher than 300 Hz. To gain a better understanding of the pipe's response, an additional measurement was conducted using four accelerometers, being one placed at the leak position and the others positioned 1, 2, and 3 meters away from the leak. The PSDs and coherence between the signals were performed and are presented in Figure 45.

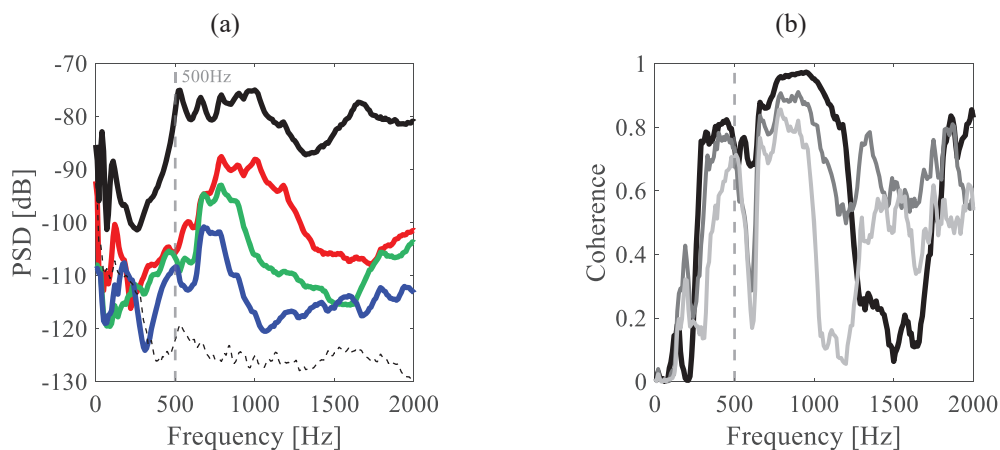


Figure 45: (a) PSDs from the Leak position (black), 1m (red), 2m (green) and 3m (blue), along with the background noise (dashed black). (b) Coherence plot between the leak and three different distance points.

It is evident that the signals exhibit the lowest amplitudes and coherence in the 0–500 Hz range, which corresponds to the bandwidth utilized by the camera. The pipe characteristics and boundary conditions result in a response where the useful bandwidth is concentrated at higher frequencies with lower amplitudes than what the camera can effectively capture. A potential solution would be to use two or more synchronized cameras positioned closer to the pipe, allowing for higher frame rates and improved spatial resolution while recording different measurement points.